

# Evidence of three-dimensional Ising ferromagnetism in the *A*-site-ordered perovskite $\text{CaCu}_3\text{Ge}_4\text{O}_{12}$

J.-G. Cheng, J.-S. Zhou,\* and J. B. Goodenough

*Materials Science and Engineering Program/Mechanical Engineering, University of Texas at Austin, Austin, Texas 78712, USA*

Y. T. Su and Y. Sui

*Center for Condensed Matter Science and Technology, Department of Physics, Harbin Institute of Technology, Harbin, 150001, China*

(Received 24 February 2011; revised manuscript received 26 April 2011; published 23 June 2011)

The *A*-site-ordered perovskite  $\text{CaCu}_3\text{Ge}_4\text{O}_{12}$  synthesized under high pressure undergoes ferromagnetic spin ordering below  $T_c \approx 12$  K. The critical exponents have been determined from isotherms of magnetization across  $T_c$  via an iteration process and the Kouvel-Fisher method as well as from specific heat. Based on fitting parameters of  $T_c$ ,  $\beta$ , and  $\gamma$ , the magnetization data in the vicinity of  $T_c$  can be scaled onto two universal curves in the plot of  $M/|t|^\beta$  vs  $H/|t|^{\beta+\gamma}$ , where  $t = T/T_c - 1$ . Critical exponents  $\alpha$ ,  $\beta$ , and  $\gamma$  obtained indicate that  $\text{CaCu}_3\text{Ge}_4\text{O}_{12}$  is a three-dimensional coupled Ising ferromagnet with a small coercivity.

DOI: [10.1103/PhysRevB.83.212403](https://doi.org/10.1103/PhysRevB.83.212403)

PACS number(s): 75.40.Cx, 75.47.Lx, 75.30.Et, 75.10.Hk

$\text{CaCu}_3\text{Ge}_4\text{O}_{12}$  crystallizes in an *A*-site 1:3 ordered cubic perovskite  $AA'_3B_4O_{12}$  with  $Im\bar{3}$  symmetry.<sup>1</sup> Figure 1(a) shows the crystal structure of  $\text{CaCu}_3\text{Ge}_4\text{O}_{12}$  by highlighting the rotations of the corner-shared  $\text{GeO}_{6/2}$  octahedra. In this  $2a_p \times 2a_p \times 2a_p$  cubic unit cell, the corner-shared  $\text{GeO}_{6/2}$  octahedra are heavily tilted, which leads to an average  $\langle \text{Ge}-\text{O}-\text{Ge} \rangle$  bond angle of  $\sim 146^\circ$ . This tilting is induced by the reduction of the 12-fold oxygen coordination of an *A* site occupied by a  $\text{Cu}^{2+}$  ion; a  $\text{Cu}^{2+}$  ion is stabilized in a square-coplanar  $\text{CuO}_4$  coordination. The  $\text{CuO}_4$  planes are oriented orthogonal to one another as illustrated in Fig. 1(b). In contrast with most magnetic transition-metal perovskites, the dominant interatomic exchange interactions are between magnetic ions on *A* sites in  $\text{CaCu}_3\text{Ge}_4\text{O}_{12}$ . Among the *A*-site-ordered perovskites  $\text{CaCu}_3B_4\text{O}_{12}$ , magnetic interactions between  $\text{Cu}^{2+}$  spins depend sensitively on the *B*-site cation.<sup>2</sup> Metallic paramagnetism has been found in the compound with  $B = \text{V}$ ,<sup>3</sup>  $\text{Co}$ ,<sup>4</sup> and  $\text{Ru}$ ,<sup>5</sup> in which a heavy-fermion state has been observed. The magnetic structures are complicated when the *B*-site cation contains localized magnetic moments such as  $\text{Mn}^{4+}$  (Ref. 6) and  $\text{Fe}^{4+}$ .<sup>7</sup> But, for nonmagnetic *B*-site cations  $\text{Ti}$ ,<sup>1</sup>  $\text{Pt}$ ,<sup>8</sup>  $\text{Ge}$ ,<sup>1</sup> and  $\text{Sn}$ ,<sup>1</sup> spin ordering on the *A*-site  $\text{Cu}^{2+}$  is antiferromagnetic for  $B = \text{Ti}$  ( $T_N = 25$  K) and  $B = \text{Pt}$  ( $T_N = 40$  K), ferromagnetic for  $B = \text{Ge}$  ( $T_c = 13$  K) and  $\text{Sn}$  ( $T_c = 10$  K). It has been argued<sup>1,8</sup> that the involvement of the  $\text{Ti}-3d^0$  and  $\text{Pt}-e_g^0$  empty orbitals produces the antiferromagnetic *Cu-O-B-O-Cu* superexchange interactions. On the other hand, the superexchange interactions through the  $100^\circ$  *Cu-O-Cu* bond indicated in Fig. 1(a) dominate where the *B*-ion orbitals are fully occupied, i.e., for  $B = \text{Ge}^{4+}$  and  $\text{Sn}^{4+}$ . The unusual bonding configuration for magnetic  $\text{Cu}^{2+}$  on *A* sites motivates us to study the critical behavior associated with the ferromagnetic transition in  $\text{CaCu}_3\text{Ge}_4\text{O}_{12}$ .

Magnetic interactions between localized spins in a crystal can be generally described by the Hamiltonian

$$H = -2J \sum_{i,j} [a S_i^z S_j^z + b (S_i^x S_j^x + S_i^y S_j^y)]. \quad (1)$$

The Hamiltonian covers the isotropic Heisenberg model ( $a = b = 1$ ), the anisotropic *XY* model ( $a = 0$ ,  $b = 1$ ), and the Ising model ( $a = 1$ ,  $b = 0$ ). Different critical exponents corresponding to these models have been derived theoretically.<sup>9</sup> In a real magnetic system, however, critical

behaviors are influenced by the energy scale of the magnetic transition temperature relative to characteristic energies like crystal-field splitting, single-ion anisotropy, and spin-orbit coupling, which makes a specific model more applicable. The Heisenberg model is more suitable for magnets with a higher transition temperature. However, the 3D Ising ferromagnet is rare in existing magnets since the spin degree of freedom is reduced. It is interesting that the critical behaviors of perovskite ferromagnet  $\text{CaCu}_3\text{Ge}_4\text{O}_{12}$  with  $T_c \approx 12$  K can be well-described by a 3D Ising model.

As reported in the literature,<sup>1</sup> polycrystalline  $\text{CaCu}_3\text{Ge}_4\text{O}_{12}$  samples in this study were prepared under high pressure and high temperature (HPHT) with a Walker-type multianvil module (Rockland Research Corp.). The precursor for HPHT synthesis was first obtained by calcining a stoichiometric mixture of  $\text{CaCO}_3$ ,  $\text{CuO}$ , and  $\text{GeO}_2$  at  $1000^\circ\text{C}$  for 24 h in air. After regrinding, the precursor was sealed in a platinum capsule that was subjected to HPHT treatment at 6 GPa and  $1000^\circ\text{C}$  for 30 min. Details about our sample assembly for HPHT synthesis can be found elsewhere.<sup>10</sup> The phase purity of the samples obtained was checked with powder x-ray diffraction (XRD) at room temperature with a Philips X'pert diffractometer ( $\text{Cu K}\alpha$  radiation). The XRD pattern recorded in the  $2\theta$  range  $15\text{--}120^\circ$  with a step size of  $0.02^\circ$  and a dwell time of 10 s has been refined in the cubic  $Im\bar{3}$  (No. 204) space group with the Rietveld method and the FullProf program;<sup>11</sup> the refinement converged very well with the reliability factors  $R_p = 3.29\%$ ,  $R_{wp} = 4.23\%$ , and  $\chi^2 = 1.27$ . The obtained lattice parameter  $a = 7.2090(1)$  Å agrees well with that of  $7.202$  Å reported by Ozaki *et al.*,<sup>12</sup> but is slightly smaller than that of  $7.26701(1)$  Å reported in Ref. 1. However, the magnetic properties of the present study are nearly identical to those reported in Ref. 1 as discussed below. We noticed that the XRD profile of our sample exhibits very sharp peaks close to the instrumental resolution. For example, the full width at half maximum (FWHM) of the main peak (220) at  $2\theta = 35.182^\circ$  is  $0.0768^\circ$ , while the instrumental broadening determined from a  $\text{LaB}_6$  standard at this angle is about  $0.078^\circ$ . Such a narrow diffraction profile indicates that the sample is not only well-crystallized, but also has a high degree of ordering of Ca and Cu ions at the *A* sites. Magnetic properties and specific heat of the high-pressure products have been measured with a superconducting quantum interference device (SQUID)

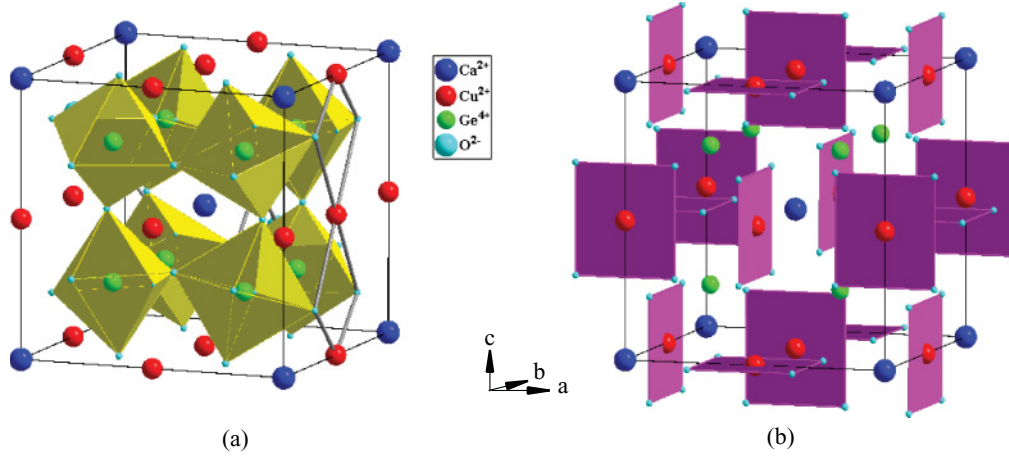


FIG. 1. (Color online) Crystal structure of  $\text{CaCu}_3\text{Ge}_4\text{O}_{12}$  by highlighting (a) the network of corner-shared  $\text{GeO}_{6/2}$  octahedra and the superexchange interatomic interaction through the  $100^\circ$  Cu-O-Cu bond and (b) the perpendicular alignment of the  $\text{CuO}_4$  planes.

magnetometer (Quantum Design) and a Physical Properties Measurement System (PPMS, Quantum Design), respectively. The temperature dependence of the magnetization  $M(T)$  measured under a magnetic field of  $H = 2000$  Oe exhibits a sharp increase at low temperatures with a sharp minimum at  $T = 12.5$  K in the temperature derivative of  $dM/dT$ ; the high-temperature Curie-Weiss fitting yields  $\mu_{\text{eff}} = 1.91 \mu_B/\text{Cu}$  and  $\theta_{\text{CW}} = 14.2$  K. The  $M(H)$  curve between  $+5$  and  $-5$  T measured at 5 K gives a saturation moment of  $1.1 \mu_B/\text{Cu}$  and a coercive force  $H_c$  smaller than 15 Oe. These results are consistent with those reported in Ref. 1. In the following, we focus on the critical behaviors of  $\text{CaCu}_3\text{Ge}_4\text{O}_{12}$  around  $T_c$ .

Figure 2(a) shows the isothermal magnetization curves  $M$  vs  $H$  of  $\text{CaCu}_3\text{Ge}_4\text{O}_{12}$  in the temperature range 9–15 K, where the demagnetization effect has been corrected. Isotherms in the  $M^2$  vs  $H/M$  plot [Fig. 2(b)] are curved, which rules out the possibil-

ity of using a mean-field model. We have analyzed the magnetization by using the general formula for the critical exponents,

$$M(T) \sim |T/T_c - 1|^\beta, \quad T < T_c, \quad (2)$$

$$\chi^{-1}(T) \sim |T/T_c - 1|^\gamma, \quad T > T_c, \quad (3)$$

$$M(H) \sim H^{1/\delta}, \quad T = T_c. \quad (4)$$

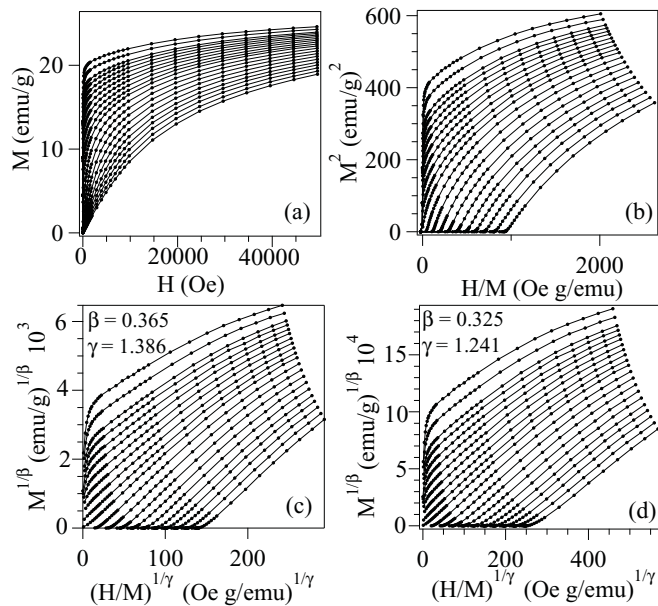


FIG. 2. (a) Isothermal magnetization curves between 9 and 15 K, and the modified Arrott plots with critical exponents of the (b) mean-field model, (c) 3D Heisenberg model, and (d) 3D Ising model.

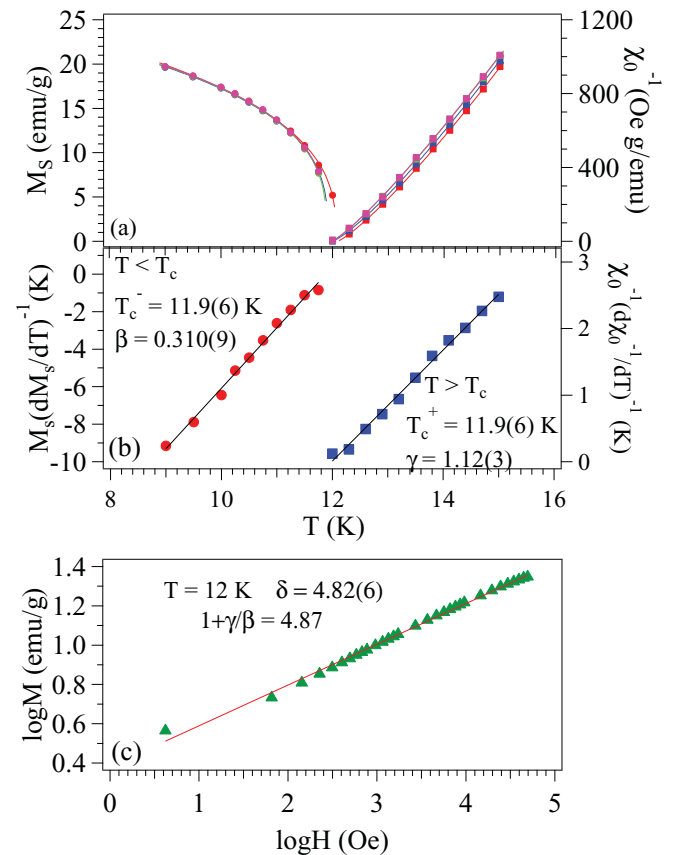


FIG. 3. (Color online) Critical exponents,  $\beta$  and  $\gamma$ , and critical temperatures,  $T_c^-$  and  $T_c^+$ , determined from (a) an iteration process started from the mean-field Arrott plot, and (b) Kouvel-Fisher plots. (c) Critical isotherms at  $T = 12$  K and the fulfillment of the Widom scaling relation (Ref. 16):  $\delta = 1 + \gamma/\beta$ .

TABLE I. Critical exponents of  $\text{CaCu}_3\text{Ge}_4\text{O}_{12}$  and theoretical values from three models.

	Ref.	$\alpha$	$\beta$	$\gamma$	$\delta$
$\text{CaCu}_3\text{Ge}_4\text{O}_{12}$	This work	0.13(2)	0.320(9)	1.20(3)	4.82(6)
Mean-field model	9	0	0.5	1.0	3.0
3D Heisenberg model	9	-0.10	0.365	1.386	4.80
3D Ising model	9	0.125	0.325	1.241	4.82

Isotherms were plotted in Figs. 2(c) and 2(d) in the modified Arrott plot  $M^{1/\beta}$  vs  $(H/M)^{1/\gamma}$  with the critical exponents of 3D Heisenberg (c) and 3D Ising (d) models. Although both the modified Arrott plots of the 3D Heisenberg and Ising models can produce roughly straight lines, a close inspection shows that the lines below and above  $T_c$  in the plot of the 3D Ising model are more parallel than those in the plot of the 3D Heisenberg model, which suggests that the ferromagnetism of  $\text{CaCu}_3\text{Ge}_4\text{O}_{12}$  could be better described with the 3D Ising model.

This conjecture has been further refined through iterations of the modified Arrott plot and formula for the critical exponents; more precise critical exponents of  $\beta$  and  $\gamma$  were obtained after the iterations converge.<sup>13,14</sup> Figure 3(a) illustrates results after three iterations. Critical exponents converged quickly to  $\beta = 0.317(5)$ ,  $\gamma = 1.18(2)$ , and  $T_c \approx 11.95$  K. Using  $M_s(T)$  and  $\chi_0^{-1}(T)$  obtained by extrapolating an isotherm to either the vertical or the horizontal axes in the modified Arrott plot with the final critical exponents, we have checked the Kouvel-Fisher (KF) relation,<sup>15</sup> viz.,

$$M_s(T)[dM_s(T)/dT]^{-1} = (T - T_c^-)/\beta, \quad (5)$$

$$\chi_0^{-1}(T)[d\chi_0^{-1}(T)/dT]^{-1} = (T - T_c^+)/\gamma. \quad (6)$$

Linear fittings to the plots of  $M_s(T)[dM_s(T)/dT]^{-1}$  and  $\chi_0^{-1}(T)[d\chi_0^{-1}(T)/dT]^{-1}$  vs  $T$  in Fig. 3(b) yield  $\beta = 0.310(9)$  and  $\gamma = 1.20(3)$ . Both values of  $\beta$  and  $\gamma$  obtained by the KF relation are quite consistent with results from the iterations of the Arrott plot and are very close to those of the 3D Ising model:  $\beta = 0.325$  and  $\gamma = 1.241$ . We also obtained the critical exponent  $\delta$  associated with the critical isotherm  $M(H)$  at  $T_c$ . The log-log plot of  $M$  vs  $H$  in Fig. 3(c) of the isotherm at  $T_c = 12$  K fits a line with  $\delta = 4.82(6)$ . Critical exponents of  $\text{CaCu}_3\text{Ge}_4\text{O}_{12}$  obtained in this study satisfy the Widom scaling relation<sup>16</sup> perfectly,  $\delta = 1 + \gamma/\beta$ . These critical exponents are listed in Table I together with those theoretical values from different models for comparison.

In order to test the reliability of our analysis for the critical behavior in  $\text{CaCu}_3\text{Ge}_4\text{O}_{12}$ , isotherms have been plotted based on the scaling hypothesis<sup>9</sup>:

$$M(H, \varepsilon) = |\varepsilon|^\beta f_\pm(H/|\varepsilon|^{\beta+\gamma}), \quad (7)$$

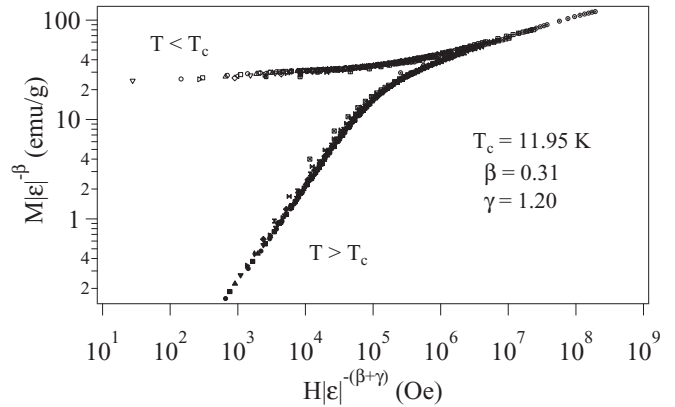


FIG. 4. Scaling plot for  $\text{CaCu}_3\text{Ge}_4\text{O}_{12}$  below and above  $T_c$  based on the critical temperature  $T_c = 11.95$  K and critical exponents  $\beta = 0.310$  and  $\gamma = 1.20$ .

where  $f_+$  for  $T > T_c$  and  $f_-$  for  $T < T_c$  are regular analytical functions, and  $\varepsilon = T/T_c - 1$  is the reduced temperature. Equation (6) implies that the  $M/|\varepsilon|^\beta$  as a function of  $H/|\varepsilon|^{\beta+\gamma}$  produces two universal curves: one for  $T < T_c$  and the other for  $T > T_c$ . By using the values of  $\beta$  and  $\gamma$  obtained by the KF method and  $T_c = 11.95$  K, we have obtained the scaled data plotted in Fig. 4; all the points indeed fall on two curves. One concern may be the residual strain effect on the critical behavior. To this end, we have checked the critical behavior from the  $\text{CaCu}_3\text{Ge}_4\text{O}_{12}$  sample annealed at 200 °C for 12 h in air in order to remove the residual strain created during HPHT synthesis. The sample exhibits the same critical behavior as that in the as-prepared sample.

A complete analysis of critical behavior should also include a thorough study of specific heat. By using the standard procedure in the PPMS, we obtained the  $C_p(T)$  of  $\text{CaCu}_3\text{Ge}_4\text{O}_{12}$ , which is identical to that in the literature.<sup>1</sup> However, data as shown in the inset of Fig. 5 collected with the finest temperature interval include limited information for tracking down the critical behavior near  $T_c$ . In order to overcome this difficulty, we have made use of a larger heat pulse and collected data while the heat pulse decays over a temperature range across  $T_c$ .<sup>17</sup> The  $C_p$  data calculated from the pulse decay are shown in Fig. 5 together with the  $C_p$  data of Ni (Ref. 18) scaled at  $T_c = 11.88$  K for comparison. A dramatic difference between the two curves occurs at  $T < T_c$ . The  $C_p$  data have been analyzed with the power-law formula<sup>19</sup> for the critical behavior,

$$C_p^+ = A^+(\varepsilon^{-\alpha^+} - 1)/\alpha^+ + B^+ + D^+\varepsilon, \quad T > T_c, \quad (8)$$

$$C_p^- = A^-(|\varepsilon|^{-\alpha^-} - 1)/\alpha^- + B^- + D^-\varepsilon, \quad T < T_c. \quad (9)$$

Whereas fitting to the  $C_p$  data of Ni gives  $\alpha = -0.087(3)$  for both  $C_p^+$  and  $C_p^-$ , characteristic of the 3D Heisenberg model, the fitting quality with a single  $\alpha$  for both  $C_p^+$  and  $C_p^-$

TABLE II. Fitting parameters in Eqs. (7) and (8) of the specific heat.

	$\log \varepsilon $	$\alpha$	$T_c$ (K)	$A$	$B$	$D$
$T < T_c$	(-2.46, -1.03)	-0.03(7)	11.883(7)	3.6(9)	19.6(1.9)	28.8(4.6)
$T > T_c$	(-3.03, -1.0)	0.13(2)	11.881(1)	2.15(23)	> 6.2(7)	-19.8(2.7)

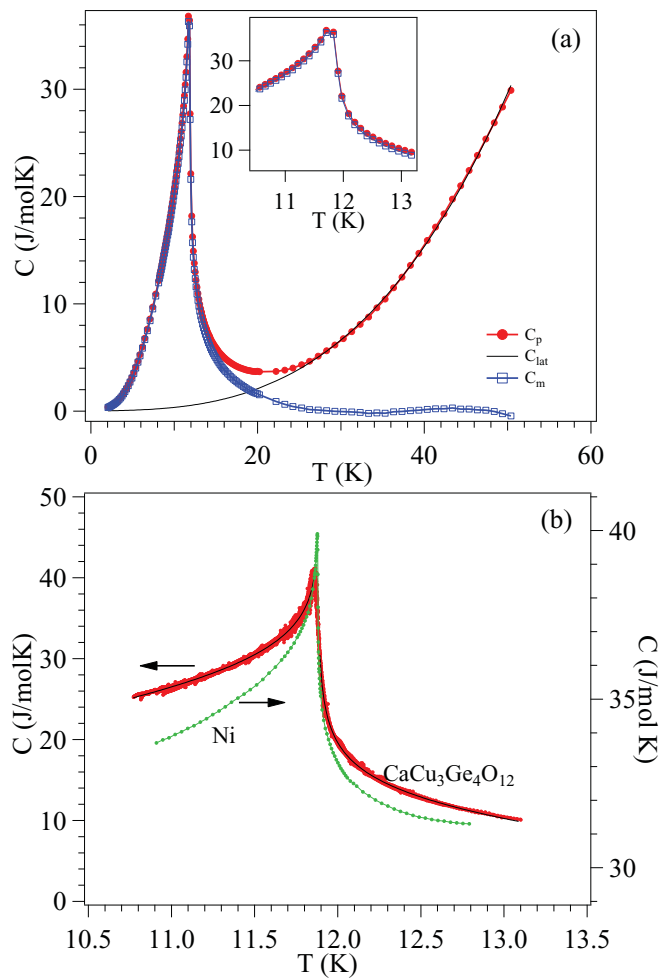


FIG. 5. (Color online) Temperature dependence of specific heat of  $\text{CaCu}_3\text{Ge}_4\text{O}_{12}$  (a) result obtained with the standard procedure for the  $C_p$  measurement in a PPMs; (b) result derived from the temperature profile during the pulse decays.

is poorer than that with two different  $\alpha$ 's for  $\text{CaCu}_3\text{Ge}_4\text{O}_{12}$ ; all parameters for the best fitting are listed in Table II. Baker<sup>20</sup> has shown theoretically that the 3D Ising model specific heat

becomes singular as  $\log|\epsilon|$  with a different coefficient above and below the singular point. Moreover,  $\alpha = 0.13(2)$  for  $C_p^+$  of  $\text{CaCu}_3\text{Ge}_4\text{O}_{12}$  fits the 3D Ising model well.<sup>9</sup>

The most studied Ising system is the magnetic dipolar ferromagnet  $\text{LiTbF}_4$ ,<sup>21</sup> where weak long-range dipole-dipole interactions dominate. The exchange interactions and an unquenched orbital angular momentum are strongly coupled to the lattice. It is therefore surprising that the critical behaviors of the perovskite  $\text{CaCu}_3\text{Ge}_4\text{O}_{12}$  can be described by a 3D Ising model since the orbital angular momentum of square-coplanar  $\text{Cu}^{2+}$  is quenched to first order and the small coercivity signals a weak coupling of the spins to the lattice. Although there is no first-order orbital angular momentum on the  $\text{Cu}^{2+}$  ion, the single  $e_g$  hole is ordered into the  $\text{CuO}_4$  planes to give a site anisotropy that would order the spins perpendicular to a  $\text{CuO}_4$  plane. But, neighboring  $\text{CuO}_4$  planes are orthogonal to one another, which gives a frustrated easy spin axis for spins aligned collinearly by a ferromagnetic  $100^\circ$  Cu-O-Cu superexchange interaction. A neutron-diffraction study<sup>22</sup> of antiferromagnetic, isostructural  $\text{CaCu}_3\text{Ti}_4\text{O}_{12}$  has indicated that the spins are oriented along a  $\langle 111 \rangle$  axis, so we assume that a  $\langle 111 \rangle$  easy axis is also the compromise for the site anisotropies of  $\text{CaCu}_3\text{Ge}_4\text{O}_{12}$ . This compromise would give strong coupling of the spins to a  $\langle 111 \rangle$  direction, but would allow easy switching between  $\langle 111 \rangle$  directions to give a low coercive force  $H_c$ . We believe it is the frustration of the site easy axes in the presence of a strong interatomic exchange interaction that is responsible for Ising critical fluctuations in a ferromagnet with small coercivity.

In conclusion, we have carried out a comprehensive study of the critical behavior associated with the ferromagnetic transition in the 1:3 A-site perovskite  $\text{CaCu}_3\text{Ge}_4\text{O}_{12}$  from the isothermal magnetization data and specific heat in the vicinity of  $T_c \approx 12$  K. The critical exponents  $\beta \approx 0.32$  and  $\gamma \approx 1.20$ , and  $\alpha \approx 0.13$  for  $C_p^+$  obtained suggest that  $\text{CaCu}_3\text{Ge}_4\text{O}_{12}$  is an extremely rare example of a 3D Ising ferromagnet having a small coercivity.

This work was supported by NSF (Grants No. DMR 0904282 and No. CBET 1048767) and the Robert A Welch foundation (Grant No. F-1066).

\*jszhou@mail.utexas.edu

<sup>1</sup>H. Shiraki *et al.*, *Phys. Rev. B* **76**, 140403 (2007).

<sup>2</sup>Y. Shimakawa, *Inorg. Chem.* **47**, 8562 (2008).

<sup>3</sup>H. Shiraki *et al.*, *J. Phys. Soc. Jpn.* **77**, 064705 (2008).

<sup>4</sup>T. Mizokawa *et al.*, *Phys. Rev. B* **80**, 125105 (2009).

<sup>5</sup>S. Tanaka *et al.*, *J. Phys. Soc. Jpn.* **78**, 024706 (2009).

<sup>6</sup>J. Sánchez-Benítez *et al.*, *Chem. Mater.* **15**, 2193 (2003).

<sup>7</sup>I. Yamada *et al.*, *Angew. Chem. Int. Ed.* **47**, 7032 (2008).

<sup>8</sup>I. Yamada *et al.*, *Inorg. Chem.* **49**, 6778 (2010).

<sup>9</sup>H. E. Stanley, *Introduction to Phase Transition and Critical Phenomena* (Oxford University Press, London, 1971).

<sup>10</sup>J.-G. Cheng *et al.*, *Phys. Rev. B* **81**, 134412 (2010).

<sup>11</sup>J. Rodríguez-Carvajal, *Physica B* **192**, 55 (1993).

<sup>12</sup>Y. Ozaki *et al.*, *Acta Cryst. B* **33**, 3615 (1977).

<sup>13</sup>F. Y. Yang *et al.*, *Phys. Rev. B* **63**, 092403 (2001).

<sup>14</sup>H. Yanagihara *et al.*, *Phys. Rev. B* **65**, 092411 (2002).

<sup>15</sup>J. S. Kouvel and M. E. Fisher, *Phys. Rev.* **136**, A1626 (1964).

<sup>16</sup>B. Widom, *J. Chem. Phys.* **41**, 1633 (1964).

<sup>17</sup>J. C. Lashley *et al.*, *Cryogenics* **43**, 369 (2003).

<sup>18</sup>D. L. Connelly *et al.*, *Phys. Rev. B* **3**, 924 (1971).

<sup>19</sup>L. W. Shacklette, *Phys. Rev. B* **9**, 3789 (1974).

<sup>20</sup>G. A. Baker, Jr., *Phys. Rev.* **129**, 99 (1963).

<sup>21</sup>L. M. Holmes *et al.*, *Phys. Rev. B* **12**, 180 (1975); J. Als-Nielsen *et al.*, *ibid.* **12**, 191 (1975); *Phys. Rev. Lett.* **32**, 610 (1974).

<sup>22</sup>Y. J. Kim *et al.*, *Solid State Commun.* **121**, 625 (2002).